Supporting Information

CuO Hollow Cubic Caves Wrapped with Biogenic N-Rich Graphitic C for Simultaneous Monitoring of Uric acid and Xanthine

Khizer Hayat [†], Aqsa Munawar [†], Anam Zulfiqar[‡], Mahmood Hassan Akhtar[§], Hafiz Badaruddin Ahmad[†*], Zahid Shafiq[†], Muhammad Akram[§], Awais Siddique Saleemi[*], Naeem Akhtar[§,**]

[†]Institute of Chemical Sciences, Bahauddin Zakariya University (BZU) Multan 60800, Pakistan

[‡]Department of Biochemistry, Bahauddin Zakariya University, (BZU) Multan 60800, Pakistan

[§]Interdisciplinary Research Centre in Biomedical Materials (IRCBM), COMSATS University Islamabad, Lahore Campus, Lahore 54000, Pakistan

[*]Institute for Advanced Study, Shenzhen University, Shenzhen 518060, Guangdong, China.

[*]Key Laboratory of Optoelectronic Devices and Systems of Ministry of Education and Guangdong Provence, College of Optoelectronic Engineering, Shenzhen University, Shenzhen 518060, Guangdong, China

Corresponding Author

Dr. Naeem Akhtar: naeemkhan@cuilahore.edu.pk
Dr. Awais Siddique Saleemi: assaleemi@szu.edu.cn
Dr. Hafiz Badaruddin Ahmad; hafizbadar@googlemail.com

Experimental Section

Characterization Techniques

The phase composition was analyzed by X-ray diffraction (XRD) measurements by using a Rigaku D/max-2550 instrument equipped with a Cu-Kα radiation source (λ=1.5418 Å). The chemical compositions and bond characters were characterized by X-ray photoelectron spectroscopy (XPS) spectra recorded on AXIS Ultra DLD spectrometer (Kratos Analytical) under ultrahigh vacuum (<10-8 Torr) and by using a monochromatic Al Kα radiations. Raman spectra were recorded on Renishaw in Via-reflex spectrometer. Static water contact angles (WCA) were measured by making thin film of material at simple glass slide. WCA was measured at room temperature by using VCA Optima, AST Products, Inc., USA. FE-SEM images were taken by using JEOL JEM model 2100F Microscope.

Result and Discussion Section

Limit of detection (LOD) and limit of quantification (LOQ)

Limit of detection (LOD) calculated by using equation S1.

$LOD = F \times SD/b$…….. (S1)

Where

F: Factor of 3.3, SD: Standard deviation of the blank, standard deviation of the ordinate intercept, or residual standard deviation of the linear regression, b: Slope of the regression line.

$LOQ = 10 \times$ standard deviation of the lower point (σ)/slop of the line…….. (S2)

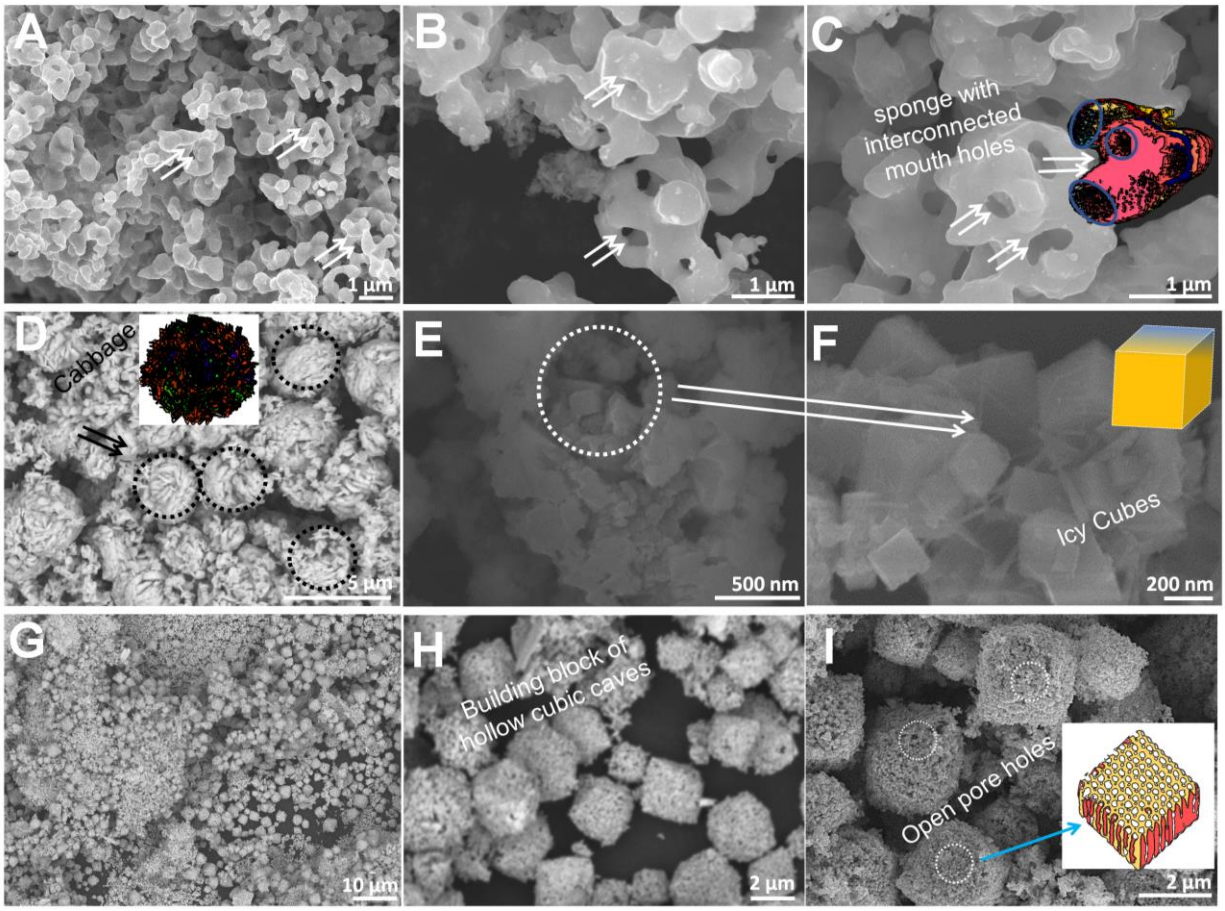

Figure S1. Low- and high-resolution SEM images of SP (A-C), CB (D), SC (E & F), HC (G & H) and NC@HC (I) showing homogenous and uniform formation of SP with interconnected holes, CB with juicy vesicles, SC with cubic morphology and HC with open pore holes containing building blocks over a wide range with uniformity and homogeneity. Image H and I shows the NC wrapped HC.

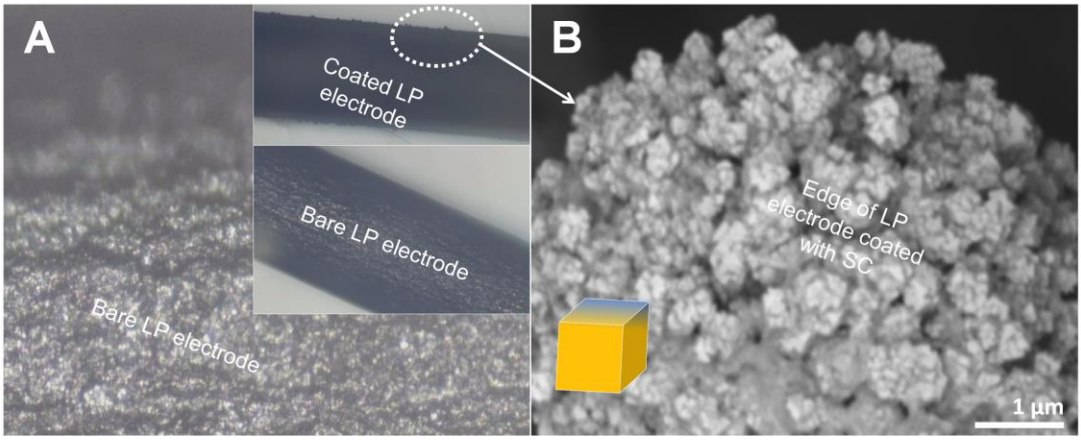

Figure S2. (A) Microscopic images of bare and coated LP electrode. SEM image showing uniform coating of SC over the tip of the LP electrode.

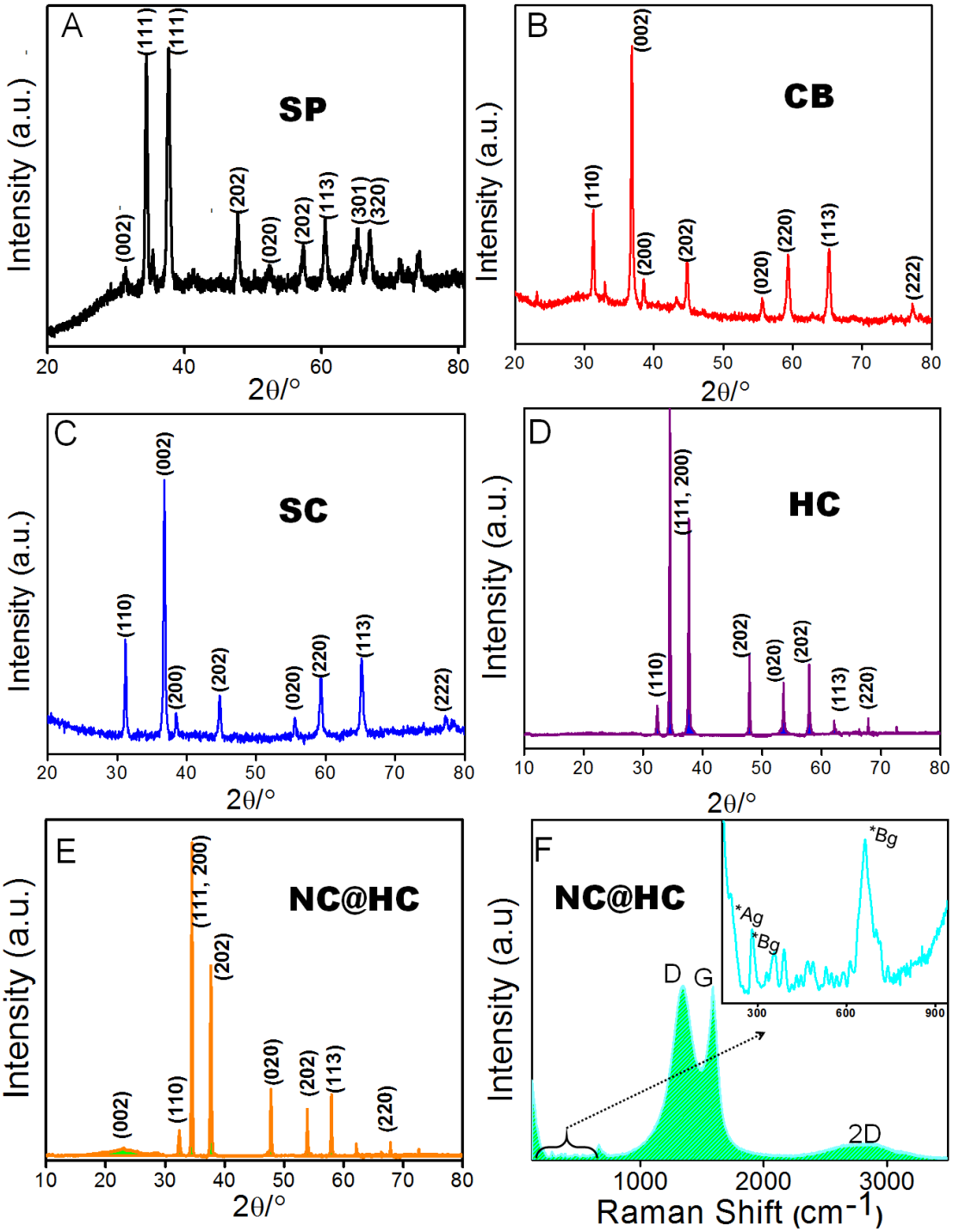

Figure S3. (A-E) XRD diffraction patterns of SP, CB, SC, HC and NC@HC, respectively. (F) Raman spectra of NC@HC with inset showing Raman active modes (Ag+2Bg).

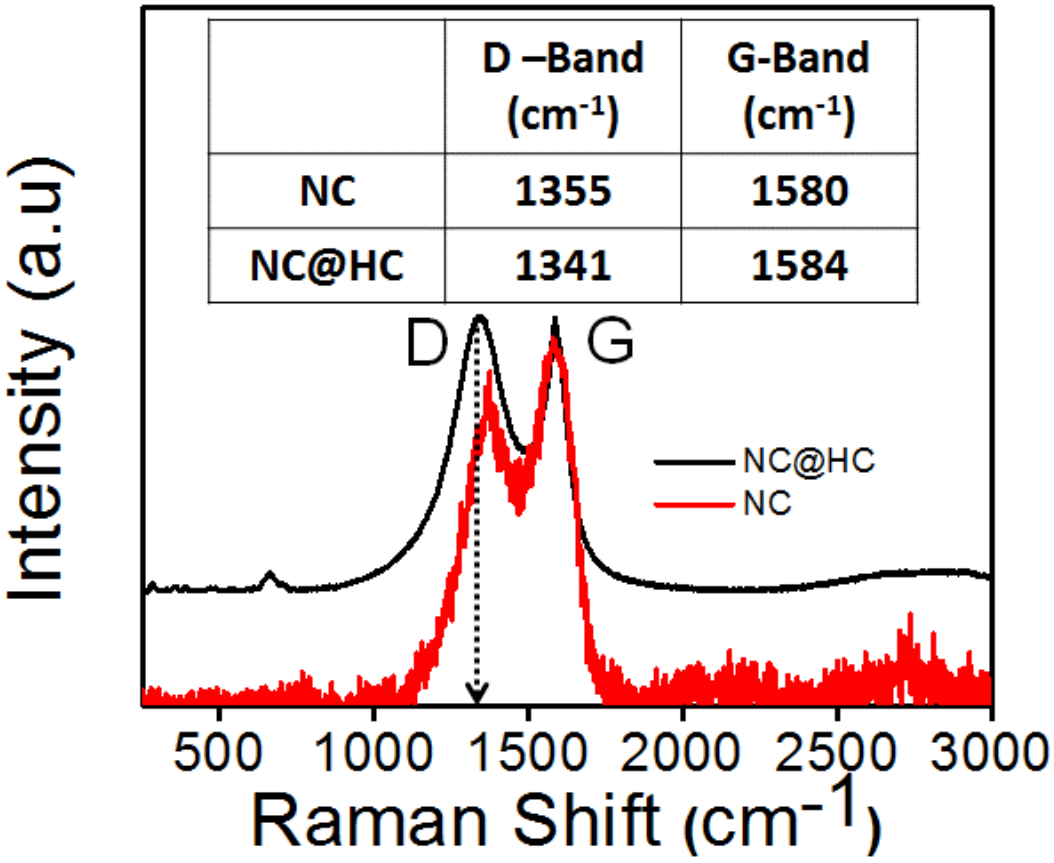

Figure S4. Raman spectra of NC@HC (red line) and NC (black line) with D and G band positions. Inset table shows a clear negative shift in D and a positive shift in G band in case of NC@HC.

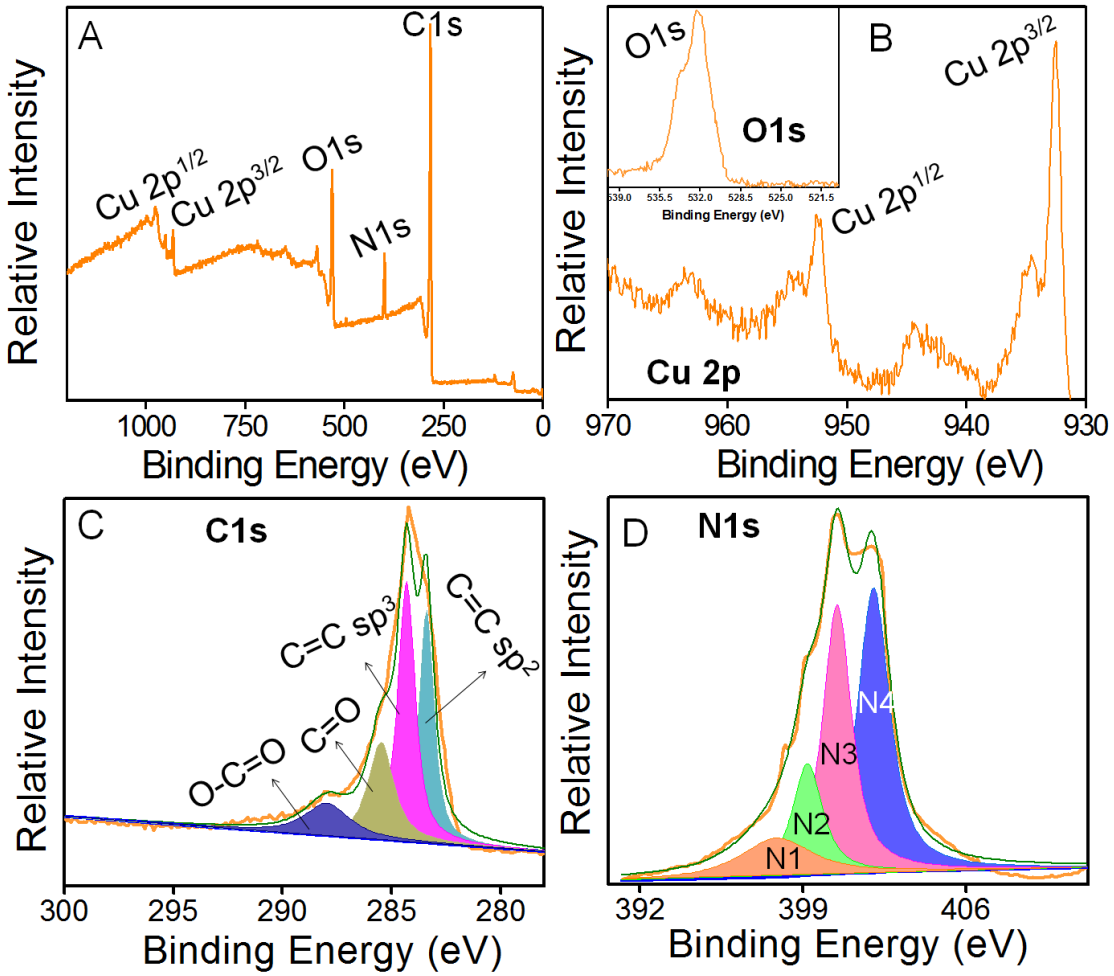

Figure S5. (A) XPS survey spectra showing the formation of NC@HC. High resolution XPS spectra of Cu (B) and presence of O (inset of B), further confirm the formation of CuO. The presence of C (C) and N (D) with deconvoluted peaks confirm their presence at the surface of HC shape CuO.

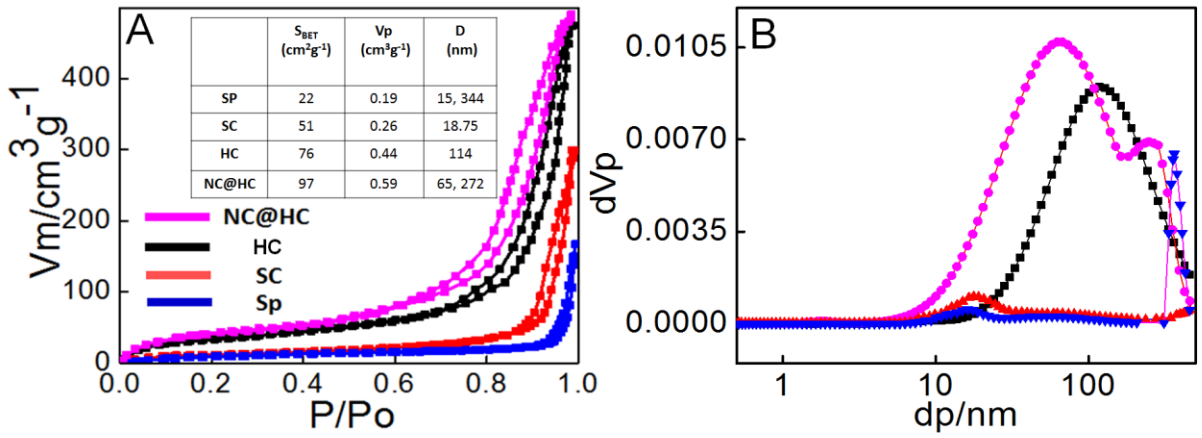

Figure S6. (A) N_2 adsorption isotherm of SP, SC, HC and NC@HC nanoparticles, whereas inset table shows their pore vole. (B) Pore volume versus pore diameter graph derived from A.

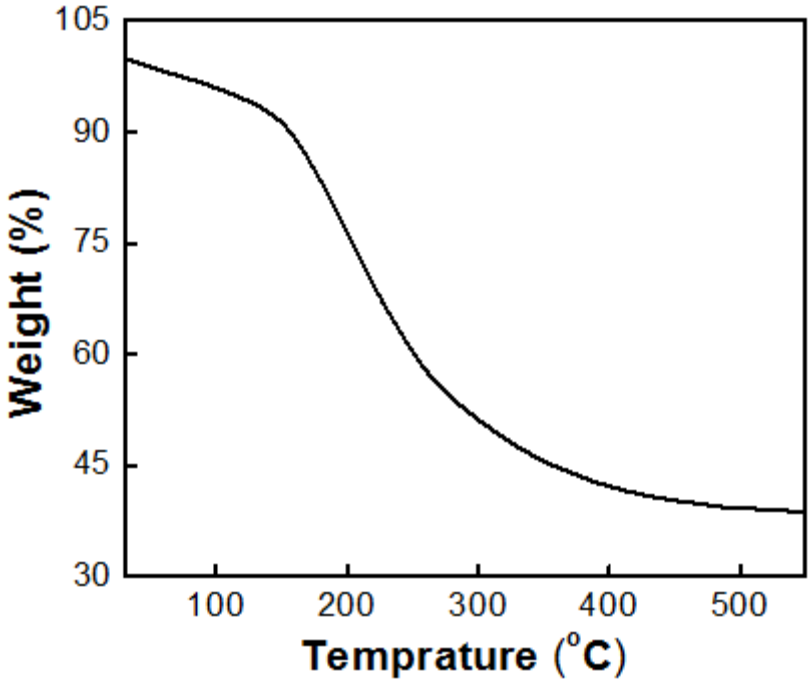

Figure S7. TGA curves of the NC@HC conducted in N_2 atmosphere within temperature range of 30–550 °C.

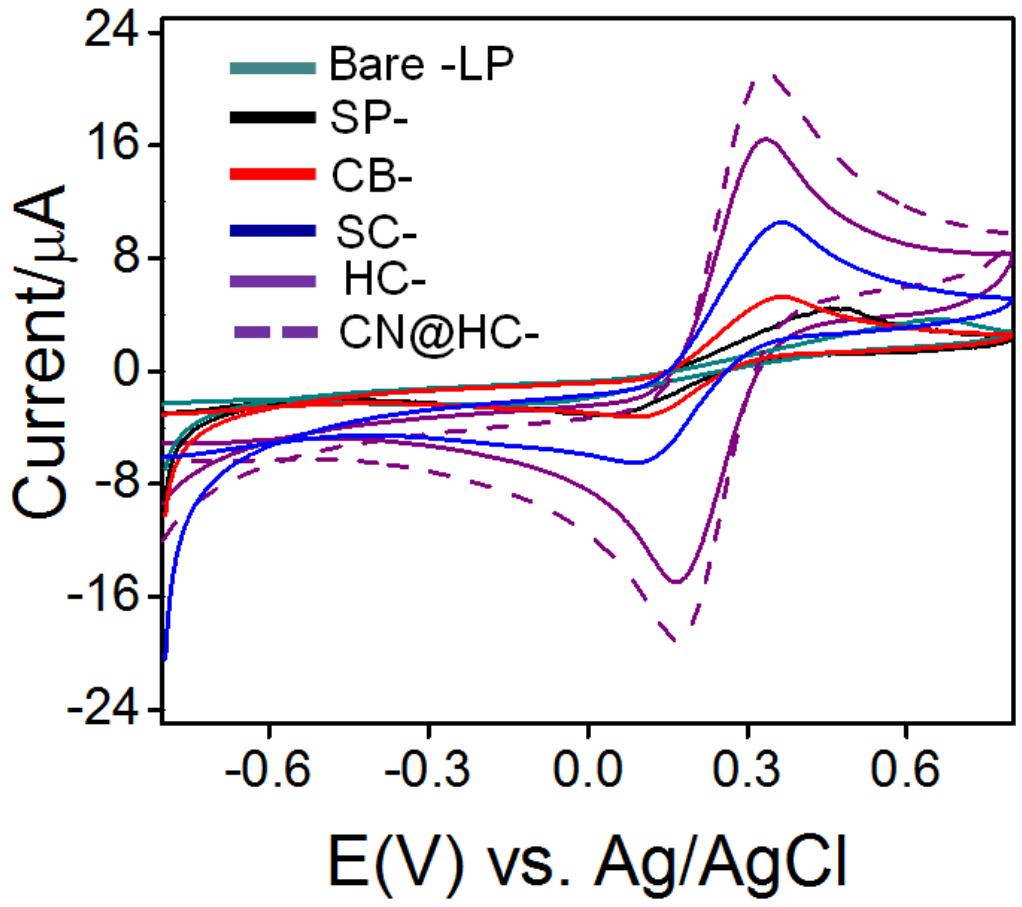

Figure S8. CV graph of bare LP, SP, CB, SC, HC and NC@HC electrode towards 2mM of $[Fe(CN)_6]^{4-/3-}$.

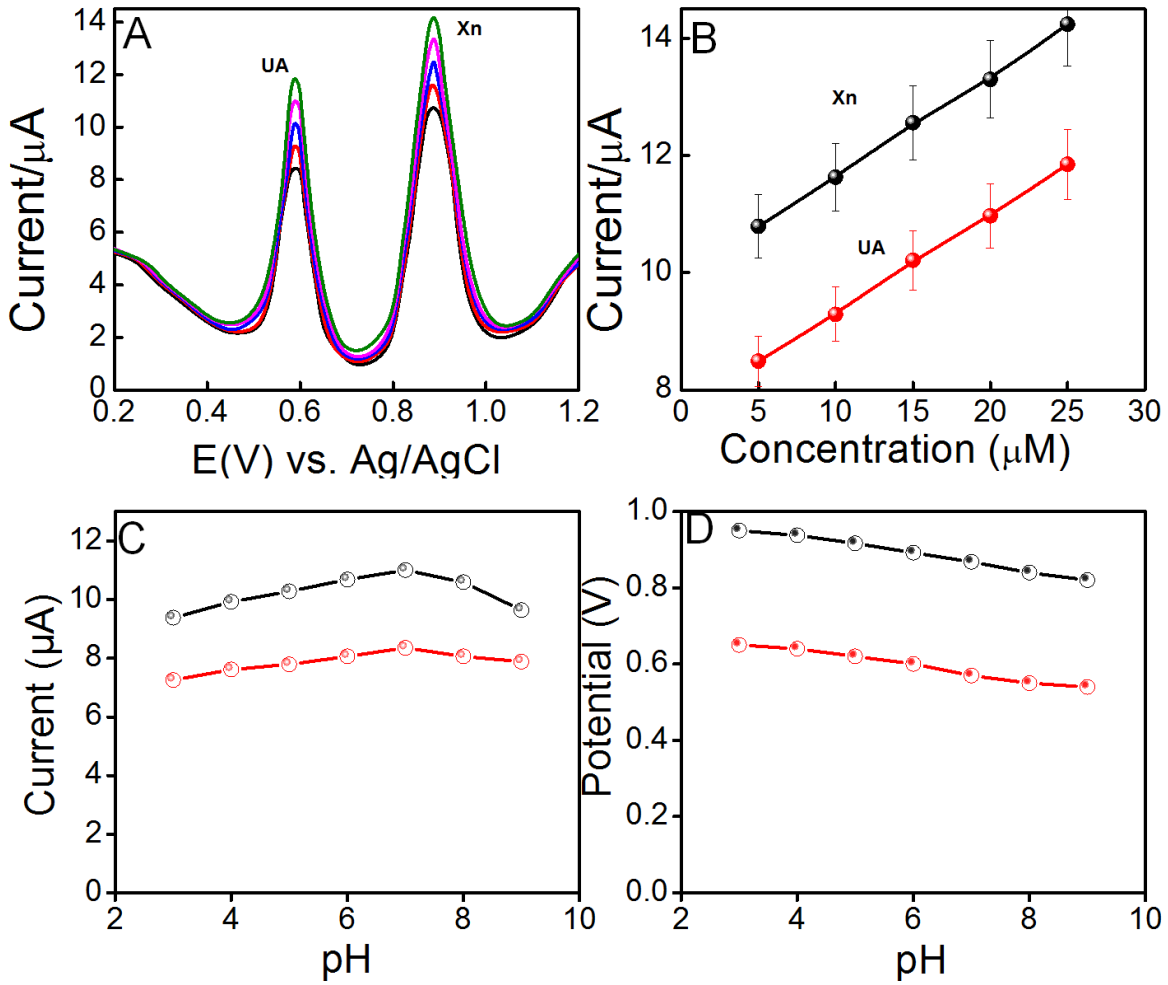

Figure S9. (A) DPV response of NC@HC electrode towards simultaneous monitoring of UA and Xn with increasing concentrations (2, 4, 6, 8 and 10 μM) in 0.1 M PBS (pH: 7.0). (B) linear plot derived from (A). (C) pH versus peak current and (D) pH versus peak potential behaviour of NC@HC electrode in 0.1 M PBS containing 2 μM of both UA and Xn.

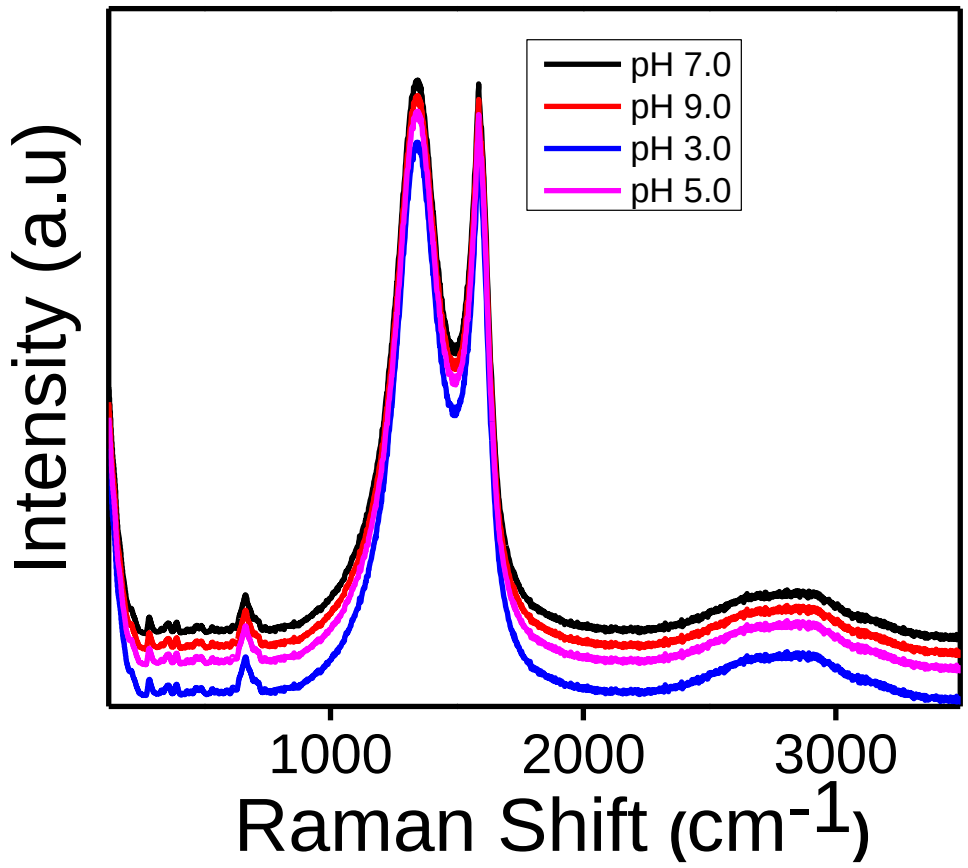

Figure S10. Raman spectra of NC@HC material exposed with three different pH including 3.0,5.0, 7.0 and 9.0 of PBS.

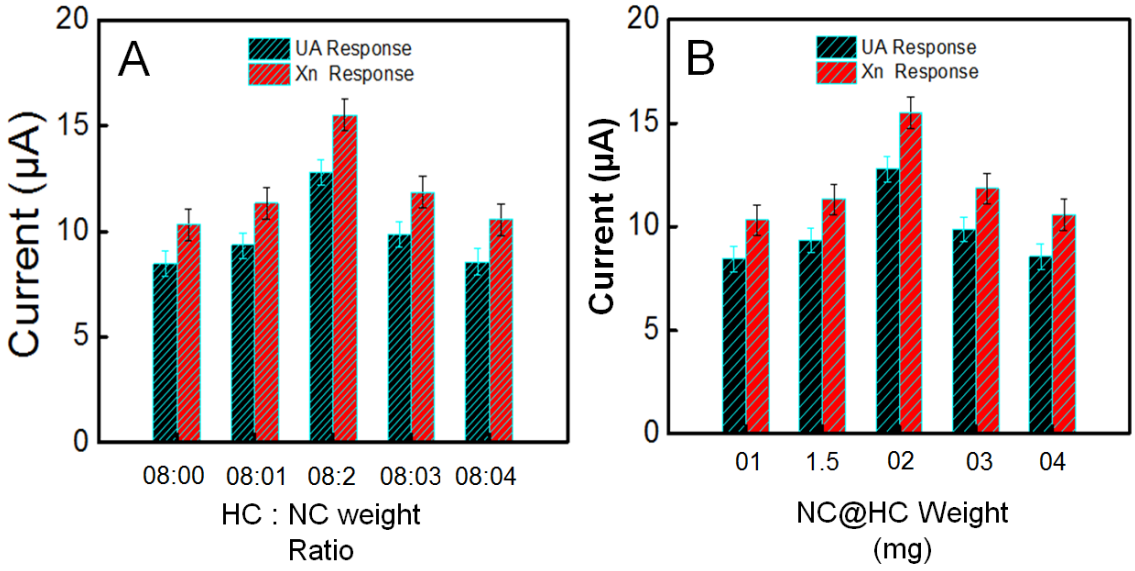

Figure S11. DPV response of NC@HC electrode towards 10 μM of UA and Xn in 0.1 M PBS (pH: 7.0) with varying (A) ratio of HC to NC and (B) loading weight of NC@HC at LP electrode.

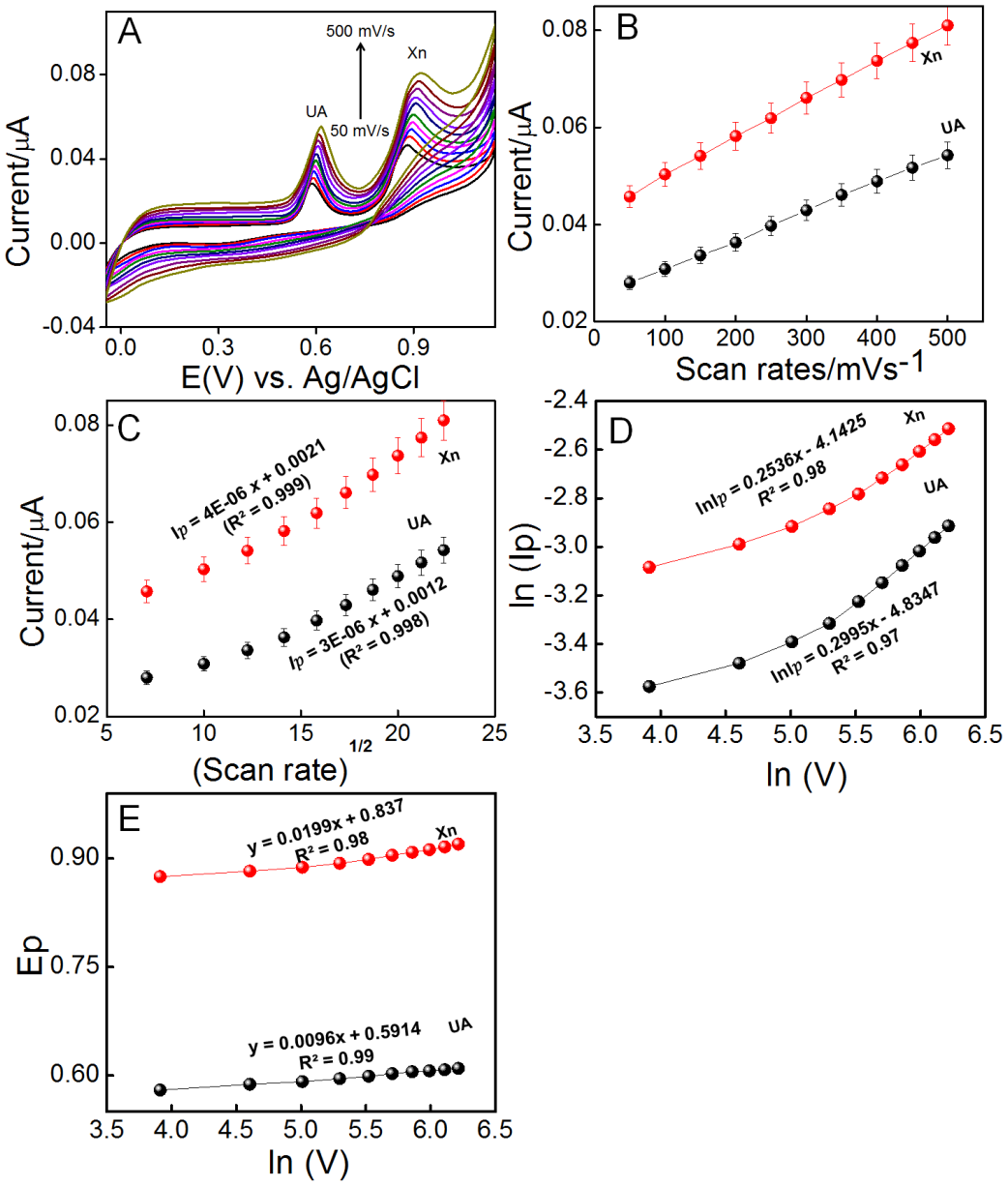

Figure S12. (A) CV patterns of NC@HC electrode towards 5 μM of UA and Xn in 0.1 M PBS with different scan rates (50-500 mV/s). Graph (B) and (C) shows relation between scan rate versus peak current and square root of scan rate versus peak current, respectively. Graph (D) and (E) shows the relation between natural log of scan rate versus natural log of peak current and natural log of scan rate versus peak potential, respectively.

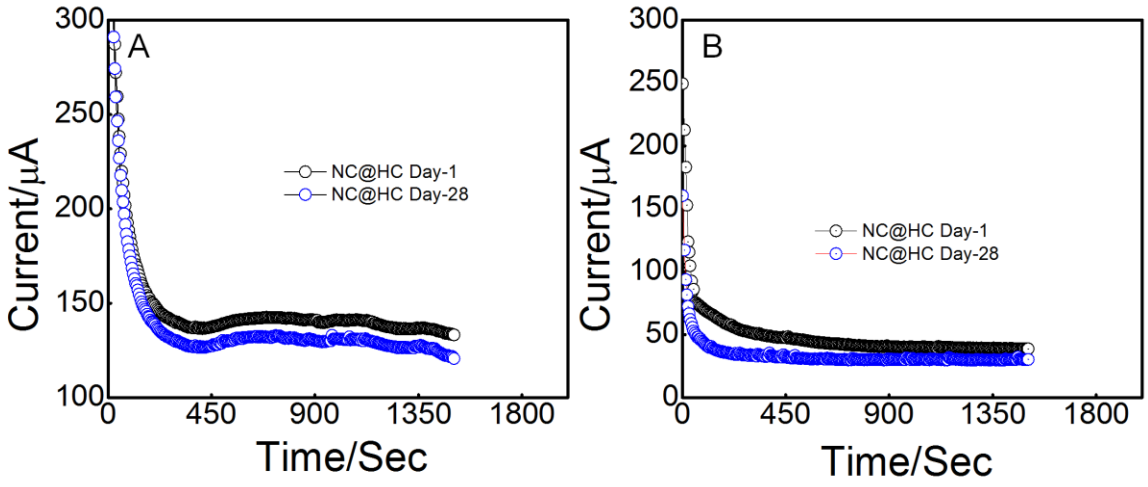

Figure S13. Chronoamperograms current response of NC@HC electrode towards (A) 50 μM of UA and (B) 05 μM of Xn at an applied potential of 0.58 and 0.88 V(vs. Ag|AgCl), respectively.

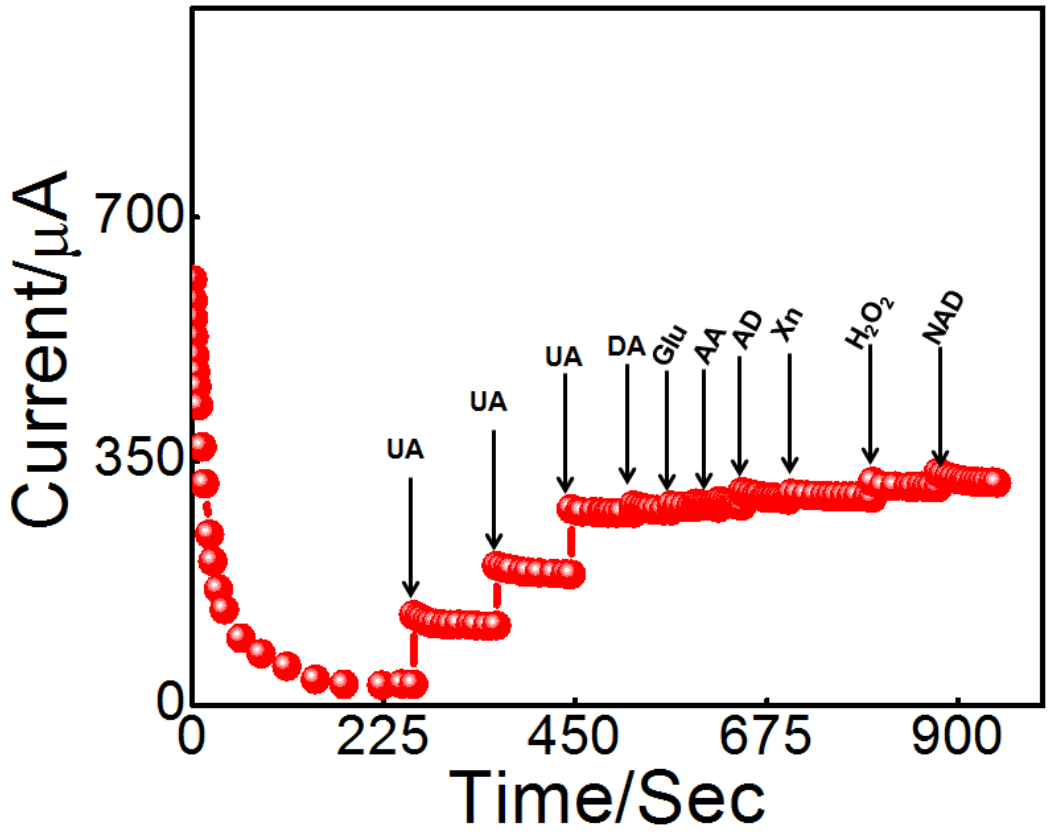

Figure S14. Amperometric selective current response of NC@HC towards 60 μM of UA (first 3 spikes only), in the presence 100μM of potentially interfering species at an applied potential of 0.58 V(vs.Ag|AgCl).

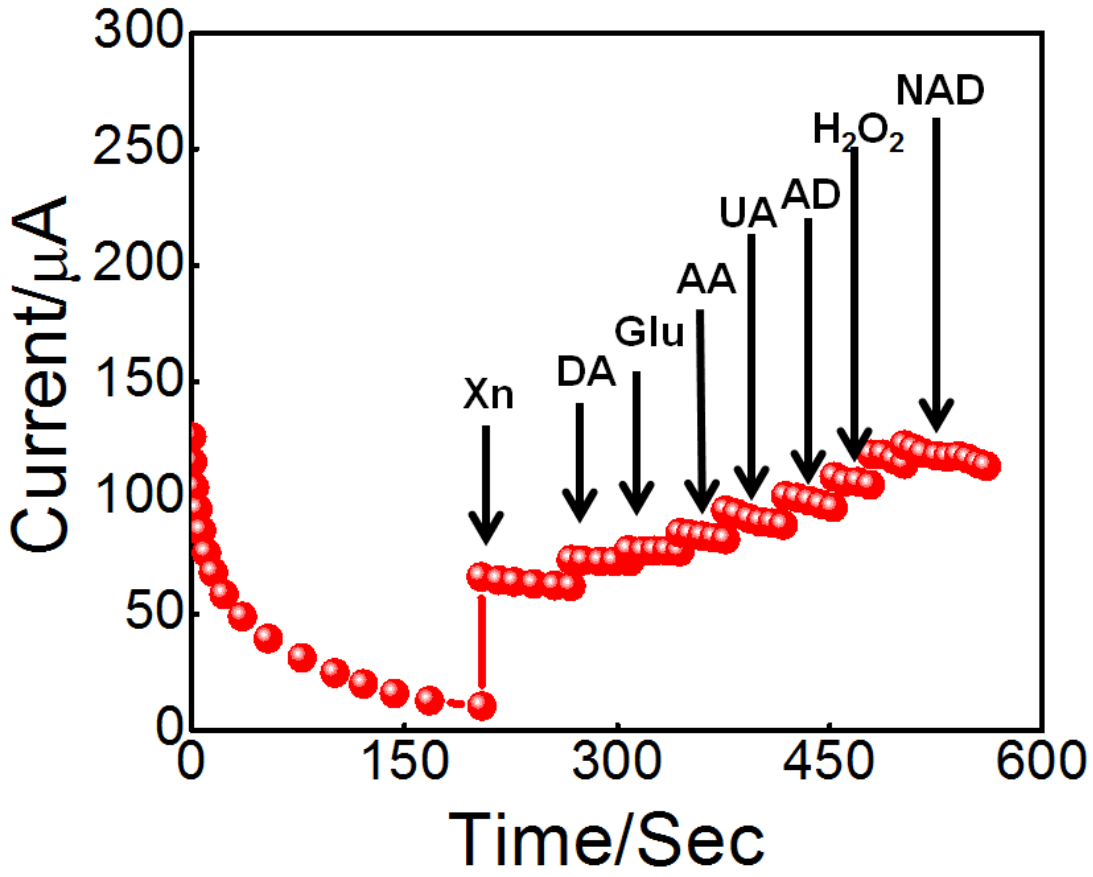

Figure S15. Amperometric selective current response of NC@HC towards 05 μM of Xn (first spikes only), in the presence 100μM of potentially interfering species at an applied potential of 0.58 and 0.88 V(vs.Ag|AgCl).

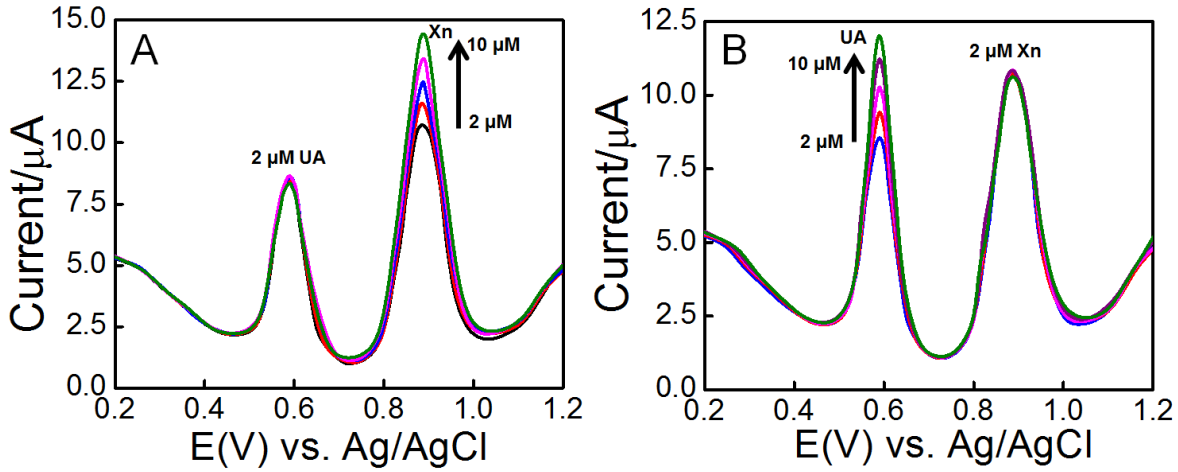

Figure S16. DPV selective response of NC@HC towards (A) constant concertation of UA (2 µM) and increasing concentration of Xn (2-10 µM), and (B) constant concertation of Xn (2 µM) and increasing concentration of UA (2-10 µM).

Table S1. Comparison in limit of detection and linear range of various sensors developed for UA and Xn with our designed NC@HC sensor.

Sr. No	Electrode	Linear range (µM)	Limit of detection (µM)	Ref.
1	Poly(L- arginine)@graphene composite film electrode	UA= 0.1- 10 XA= 0.1- 10	UA= 0.05 XA= 0.05	S 1
2	Poly(L-methionine)/GCE	UA= 0.02 -0.1 XA= 0.02 -0.1	UA= 0.0074 XA= 0.004	S 2
3	[1]BCP/GCE	UA= 0.5 - 120 XA= 0.1 -100	UA= 0.2 XA= 0.06	S 3
4	Ru $(DMSO)_4Cl_2$ Nafion membrane electrode	UA= 100 - 700 XA= 50 - 500	UA= 0.372 XA= 2.35	S 4

5	Poly (pyrocatechol violet)@ MWCNT composite film electrode	UA= 0.3- 80 XA= 0.1-100	UA= 0.16 XA= 0.05	S 5
6	[2]p-ATD@GCE	UA= 10 - 100 XA= 10 - 100	UA= 0.19 XA= 0.59	S 6
7	[3]PDAox-PTCA@GCE	UA= 1.8 - 238 XA= 5.1 - 289	UA= 0.6 XA= 1.7	S 7
8	[4]NSPE	UA= 2 - 40 XA= 2 - 40	UA= 0.42 XA= 0.07	S 8
9	[5]P6-TG/GCE	UA= 2-1600 XA= 1-500	UA= 0.06 XA= 0.3	S 9
10	[6]NG/GCE	UA= 9-1000 XA= 8-800	UA= 0.33 XA= 0.083	S 10
11	Co-CeO_2/GCE	UA= 1-2200 XA= 0.1 -1000	UA= 0.12 XA= 0.096	S 11
12	4B-PGE	UA= 3-21 XA= 8 -36	UA= 0.17 XA= 0.4	S 12
13	HAD/ErGO/GCE	UA= 5-1000 XA= 5 -300	UA= 0.08 XA= 0.1	S 13
14	NC@HC	UA= 50-1050 XA= 05-90	UA= 0.017 XA= 0.004	This work

[1]BCP = Poly (bromocresol purple)
[2]p-ATD = 2- amino thiadiazole
3PDAox-PTCA = polymer dopamine oxidase-3,4,9,10 perylenetetracarboxylic acid
[4]NSPE = Nontronitecoated screen printed electrode
[5]P6-TG = Purine based polymer
[6]NG = sulfonic group functionalized nitrogen doped graphene

Table S2. Determination of UA from real time serum sample of gout patient using developed NC@HC electrode at room conditions in 0.1 M PBS through amperometric current response.

Real Sample	Calibrated Concentration	Amperometric Current (µA) of standard (25 µM) sample at 0.62 V	Measured Current (µA) with Real Urine Sample	Respective Concentration (µM)
Serum	0.020 to 0.025 mM	56.4	66.18	29.3

Table S3. Determination of Xn from real time human urine sample using developed NC@HC electrode at room conditions in 0.1 M PBS through amperometric current response.

Real Sample	Calibrated Concentration	Amperometric Current (µA) of standard (20 µM) sample at 0.85 V	Measured Current (µA) with Real Urine Sample	Respective Concentration (µM)
Urine	0.02 to 0.025 mM	109.11	101.26	18.5

References

(S 1) Pereira, F.; Fogg, A.; Zanoni, M. V. B. Regeneration of poly-L-lysine modified carbon electrodes in the accumulation and cathodic stripping voltammetric determination of the cromoglycate anion. *Talanta* **2003,** *60* (5), 1023-1032.

(S 2) Ojani, R.; Alinezhad, A.; Abedi, Z. A highly sensitive electrochemical sensor for simultaneous detection of uric acid, xanthine and hypoxanthine based on poly (l-methionine) modified glassy carbon electrode. *Sensors and Actuators B: Chemical* **2013,** *188*, 621-630.

(S 3) Raoof, J. B.; Ojani, R.; Baghayeri, M.; Ahmadi, F. Fabrication of a fast, simple and sensitive voltammetric sensor for the simultaneous determination of 4-aminohippuric acid and uric acid using a functionalized multi-walled carbon nanotube modified glassy carbon electrode. *Analytical Methods* **2012,** *4* (6), 1825-1832.

(S 4) Kumar, A. S.; Swetha, P. Ru (DMSO) 4Cl2 nano-aggregated Nafion membrane modified electrode for simultaneous electrochemical detection of hypoxanthine, xanthine and uric acid. *Journal of Electroanalytical Chemistry* **2010,** *642* (2), 135-142.

(S 5) Sun, D.; Zhang, Y.; Wang, F.; Wu, K.; Chen, J.; Zhou, Y. Electrochemical sensor for simultaneous detection of ascorbic acid, uric acid and xanthine based on the surface enhancement effect of mesoporous silica. *Sensors and Actuators B: Chemical* **2009,** *141* (2), 641-645.

(S 6) Kalimuthu, P.; John, S. A. Simultaneous determination of ascorbic acid, dopamine, uric acid and xanthine using a nanostructured polymer film modified electrode. *Talanta* **2010,** *80* (5), 1686-1691.

(S 7) Liu, X.; Ou, X.; Lu, Q.; Zhang, J.; Chen, S.; Wei, S. Electrochemical sensor based on overoxidized dopamine polymer and 3, 4, 9, 10-perylenetetracarboxylic acid for simultaneous determination of ascorbic acid, dopamine, uric acid, xanthine and hypoxanthine. *RSC Advances* **2014,** *4* (80), 42632-42637.

(S 8) Zen, J.-M.; Lai, Y.-Y.; Yang, H.-H.; Kumar, A. S. Multianalyte sensor for the simultaneous determination of hypoxanthine, xanthine and uric acid based on a preanodized nontronite-coated screen-printed electrode. *Sensors and Actuators B: Chemical* **2002,** *84* (2-3), 237-244.

(S 9) Lan, D.; Zhang, L. Electrochemical synthesis of a novel purine-based polymer and its use for the simultaneous determination of dopamine, uric acid, xanthine and hypoxanthine. *Journal of Electroanalytical Chemistry* **2015,** *757*, 107-115.

(S 10) Luo, A.; Lian, Q.; An, Z.; Li, Z.; Guo, Y.; Zhang, D.; Xue, Z.; Zhou, X.; Lu, X. Simultaneous determination of uric acid, xanthine and hypoxanthine based on sulfonic groups functionalized nitrogen-doped graphene. *Journal of Electroanalytical Chemistry* **2015,** *756*, 22-29.

(S 11) Lavanya, N.; Sekar, C.; Murugan, R.; Ravi, G. An ultrasensitive electrochemical sensor for simultaneous determination of xanthine, hypoxanthine and uric acid based on Co doped CeO2 nanoparticles. *Materials Science and Engineering: C* **2016,** *65*, 278-286.

(S 12) Vishnu, N.; Gandhi, M.; Rajagopal, D.; Kumar, A. S. Pencil graphite as an elegant electrochemical sensor for separation-free and simultaneous sensing of hypoxanthine, xanthine and uric acid in fish samples. *Analytical Methods* **2017,** *9* (15), 2265-2274.

(S 13) Raj, M. A.; John, S. A. Simultaneous determination of uric acid, xanthine, hypoxanthine and caffeine in human blood serum and urine samples using electrochemically reduced graphene oxide modified electrode. *Analytica chimica acta* **2013,** *771*, 14-20.